

# Chaotic Convolutional Long Short-Term Memory Network for Respiratory Motion Prediction

Narges Ghasemi<sup>1,2</sup><sup>a</sup>, Shahabedin Nabavi<sup>1</sup><sup>b</sup>, Mohsen Ebrahimi Moghaddam<sup>1</sup><sup>c</sup>  
and Yasser Shekofteh<sup>1</sup><sup>d</sup>

<sup>1</sup>Faculty of Computer Science and Engineering, Shahid Beheshti University, Tehran, Iran

<sup>2</sup>Department of Computer Science, Viterbi School of Engineering, University of Southern California, U.S.A.

**Keywords:** Convolutional Long Short-Term Memory, Deep Neural Network, Lung Motion, Radiotherapy, Respiratory Motion Prediction.

**Abstract:** One of the challenges of treating lung tumors in radiation therapy is the patient's respiratory movements during the treatment, which lead to tumor motion. The goal of respiratory motion prediction is to predict the movements of lung tissues and lung tumors during the breathing cycle. Predicting respiratory movements allows radiation to be directed only at the tumor, minimizing exposure to healthy tissue and reducing the risk of side effects. Using 4D CT images, we can find the next position of the lung tumor and make a 4D radiation therapy plan. As obtaining 4D CT scans is harmful to the patient due to radiation, the aim of this study is to construct a 4D CT during a respiratory cycle using only a 3D image. In this paper, a Chaotic Convolutional Long Short-Term Memory network is proposed, which utilizes chaotic features in respiratory signals to predict pulmonary movements more accurately. The innovation of this method is paying attention to chaotic features of respiratory signals, which leads to better interpretability of the presented model. The obtained results show that the proposed method has a higher learning speed and better performance compared to previous models, which generate 4D CT scans.

## 1 INTRODUCTION


Cancer Statistics 2022 reports that lung cancer remains the foremost cause of cancer-related mortality (Siegel et al., 2022), underlining the pressing need for precise and effective treatments. Radiation therapy, which employs high-energy rays to destroy cancer cells and shrink tumors, is a fundamental part of lung cancer treatment. However, a significant challenge arises during the delivery of radiation therapy: as patients breathe, the consequent movement of tumors leads to inadvertent exposure of healthy tissue to therapeutic rays. This not only increases the risk of secondary cancers but also complicates the effective targeting of lung tumors.


Respiratory motion prediction aims to predict how lung tissues and lung tumors will move during breathing. By integrating these predictions into treatment


planning, the precision in targeting tumors can be significantly enhanced. Radiation therapists are then able to tailor the treatment plan to synchronize with the tumor's movement, ensuring that the radiation is delivered effectively to the intended target. The ability to concentrate radiation on the tumor, while limiting exposure to healthy tissue, is crucial for reducing side effects. This precision is especially important because radiation therapy, if not meticulously targeted, can inadvertently harm nearby healthy tissues.


Efficient delivery of radiation, guided by accurate prediction of pulmonary movements, can shorten the duration of treatment sessions. This is of particular importance for patients who face challenges enduring lengthy treatments. Moreover, by precisely predicting the movement of lung tissues, radiation therapists can reduce the need for multiple treatment sessions that may arise from initial targeting inaccuracies. This not only improves the efficacy of the therapy but also significantly enhances patient comfort by lessening the overall treatment burden.

A series of three-dimensional Computed Tomography (CT) scan images of the lung during the phases

<sup>a</sup> <https://orcid.org/0009-0006-6673-7760>

<sup>b</sup> <https://orcid.org/0000-0001-7240-0239>

<sup>c</sup> <https://orcid.org/0000-0002-7391-508X>

<sup>d</sup> <https://orcid.org/0000-0002-6733-3702>

of the respiratory cycle constitute a four-dimensional (4D) CT scan. Essentially, a 4D CT scan compiles multiple three-dimensional CT scans, each capturing a different phase of respiration, to provide a time-sequenced view of the lungs. This imaging technique allows clinicians to observe the internal dynamics of the body over time, which is invaluable in planning treatment by considering the shape and movement of the tumor and surrounding organs during the breathing cycle. 4D CT scan images are a valuable tool for estimating uncertainties related to respiratory movements (Rehailia-Blanchard et al., 2019). In this paper, we aim to propose a respiratory motion prediction deep learning model that considers the inherent characteristics of respiratory signals to predict future slices of a lung CT volume based on the current slices in the breathing cycle.

The contributions of this study are:

- A convolutional LSTM network architecture is proposed in this study for respiratory motion prediction to predict future slices in the breathing cycle using current slices. Using this method and 4D CT images as ground truth, the proposed model predicts the slices of the next respiratory phase volume and compares it with its corresponding slice.

- A chaotic feature extractor (CFE) and a chaotic activation function (CAF) are used to improve the prediction procedure and increase the accuracy of radiation therapy. A chaotic convolutional LSTM model is proposed to this end.

The rest of this article is organized as follows. Section 2 reviews related studies. Section 3 describes the proposed method. The results of the experiments are presented in Section 4. Section 5 discusses the results obtained, followed by the conclusion in Section 6.

## 2 RELATED WORKS

Accurate respiratory motion prediction is crucial for effective radiation treatment planning. Traditional methods, such as those using external surrogates marked on the chest or abdomen, have laid the groundwork for capturing respiratory patterns. These methods include predictive techniques based on the autoregressive moving average method (McCall and Jeraj, 2007), Kalman filter-based approaches (Lee et al., 2011; Bukhari and Hong, 2014), and kernel estimation methods (Ruan, 2010). While valuable for their non-invasiveness, they fall short in detailing the complex internal organ motions that are vital for precision in modern medical imaging techniques.

With the advent of machine learning, more so-

phisticated approaches have emerged to surmount the limitations of traditional methods. Techniques ranging from Adaptive Neuro-Fuzzy Inference Systems (Rostampour et al., 2018) to Artificial Neural Networks (ANNs) (Sun et al., 2017), and further to Recurrent Neural Networks (RNNs) (Kai et al., 2018), have been explored for their capacity to factor in the temporal dependencies missing from ANNs. The evolution of RNNs into Long Short-Term Memory (LSTMs) networks has specifically addressed the gradient vanishing and explosion challenges characteristic of earlier RNNs. In the domain of respiratory motion prediction, these LSTM networks, particularly when trained on 4D CT imaging data, have shown promise in enhancing prediction accuracy for treatment planning (Lin et al., 2019). Additionally, research has highlighted the potential of Conditional Generative Adversarial Networks (CGANs), such as the work of (Isola et al., 2017), originally designed for image-to-image translation, in next frame prediction tasks, including applications in respiratory motion prediction for medical imaging.

In the work of (Nabavi et al., 2020), the ConvLSTM-based PredNet model, initially presented in (Lotter et al., 2016) for predicting successive frames in video sequences, has been adapted for forecasting subsequent slices in medical imaging. This model leverages the existing slices as inputs to anticipate future slices in a sequence. Additionally, work of (Ghasemi and Samadi Miandoab, 2022) employs parallelized ConvLSTM layers to enhance feature extraction from the data slices, improving the predictive capabilities of the model. Our study seeks to bridge this gap by introducing a novel chaotic feature extractor (CFE) and a chaotic activation function (CAF) within the ConvLSTM framework. These additions are specifically designed to grapple with the unpredictable, chaotic nature of respiratory movement. By doing so, our model ventures beyond existing models, leveraging the chaotic dynamics of respiratory motion to potentially elevate the accuracy of predictions and adaptability to the unique breathing patterns of patients.

## 3 METHOD

The Method section is organized into three primary parts. First, we lay out the problem formulation. The second part details the proposed method, and the final part describes the implementation details and settings, offering insight into how the model is applied and tested.

### 3.1 Problem Formulation

In this study, we approach the prediction of respiratory motion using 4D CT data to infer the future state of lung CT volumes. We seek to calculate the lung CT volume at a future time point  $t + \Delta t$  based on the current volume at time  $t$ . Our model works by predicting each corresponding slice of the future CT volume,  $\hat{s}_{i+\Delta t}$ , from the current CT volume slice,  $s_i$ , and then reconstructing the complete future volume  $\hat{V}_{t+\Delta t}$ . The prediction for each slice at a given time step  $t$  and slice  $s_i$  is formulated as:

$$\hat{s}_{i+\Delta t} = f(s_i) \quad (1)$$

where  $f$  denotes the motion prediction model.

### 3.2 Proposed Method

The input of the model is the current CT volume, and we aim to predict the CT volume at the next time step. These volumes are sliced, and the input of the model is a slice of the current volume, aiming to predict the corresponding slice in the next time step. Initially, a chaotic feature extractor generates a feature map with dimensions similar to the input image. This feature map is then concatenated with the input image, followed by a convolution operation that reduces the channel size to one, merging the information of the image and the chaotic features. ConvLSTM blocks, interlaced with chaotic activation functions, further extract features, and a final convolution block generates the predicted future slice. Batch Normalization is applied between ConvLSTM blocks to enhance training speed. The architecture of the proposed framework is illustrated in Figure 1.

Chaos is characterized by seemingly irregular, unpredictable long-term, and non-periodic behavior within a deterministic system. Research of (Michalski et al., 2014) has demonstrated that respiratory signals exhibit complex nonlinear dynamics and chaotic behavior. To explore this chaotic behavior in lung CT scans, a 2D discrete cosine transform (2D DCT) is computed on the input image. The image is then traversed in a zigzag pattern from the bottom right to the top left, forming a 1D vector. This vector is subjected to a chaos test (Gottwald and Melbourne, 2004), verifying its chaotic properties.

#### 3.2.1 Chaotic Feature Extractor

Artificial intelligence has achieved remarkable success in practical applications, yet it often lacks a close representation of the chaotic firing properties observed in biological neurons. This limitation has spurred the development of neuron architectures that

embody intrinsic chaos, as seen in biological systems. In (Harikrishnan and Nagaraj, 2019; Balakrishnan et al., 2019), a single-layer chaos-inspired neuronal architecture for classification problems is proposed. In our research, the Generalized Luröth Series (GLS) neurons form the input layer, consisting of  $n$  neurons  $G_1, G_2, \dots, G_n$ , where  $n$  is the length of the vectorized input image, and the pixel values are normalized to the interval  $[0, 1]$ .

The GLS neuron is described by a 1-D piecewise linear chaotic map  $T : [0, 1) \rightarrow [0, 1)$ , given by:

$$T(x) = \begin{cases} \frac{x}{b} & \text{if } 0 \leq x < b \\ \frac{1-x}{1-b} & \text{if } b \leq x < 1 \end{cases} \quad (2)$$

where  $x$  lies in the range  $[0, 1)$ . The parameter  $b$  is a crucial component of the GLS map, influencing the neuron's chaotic behavior. In this study, the value of  $b$  was determined through empirical testing. Various values were trialed, and the optimal  $b$  was selected based on the performance of the model.

Each GLS neuron starts with an initial neural activity  $q$ , representing the initial value for the chaotic map. These neurons then fire chaotically in response to a stimulus, a real number between 0 and 1. The firing time—or the number of iterations required for the neuron's output to fall within an epsilon neighborhood of the pixel's initial value—is used as the chaotic feature for that particular pixel. The concept of Topological Transitivity (TT) ensures that this process will converge, meaning that firing will eventually cease, as demonstrated in (Harikrishnan and Nagaraj, 2019; Balakrishnan et al., 2019).

The features extracted by this method, now in vector form, are then reshaped to match the input image's dimensions and concatenated back to the input image for further processing.

#### 3.2.2 Convolutional Long Short-Term Memory

The 4D CT captures the movement of the organs and tumor over time. It consists of a sequence of 3D CTs. In order to take advantage of the temporal dependency between images, we can use long short-term memory that is created to predict time series. The main drawback of long short-term memory is not paying attention to the spatial characteristics of the data because it loses the spatial properties by vectorizing the data. This problem can be overcome by using convolutional long short-term memory, which is designed for spatiotemporal sequence forecasting problems (Shi et al., 2015).

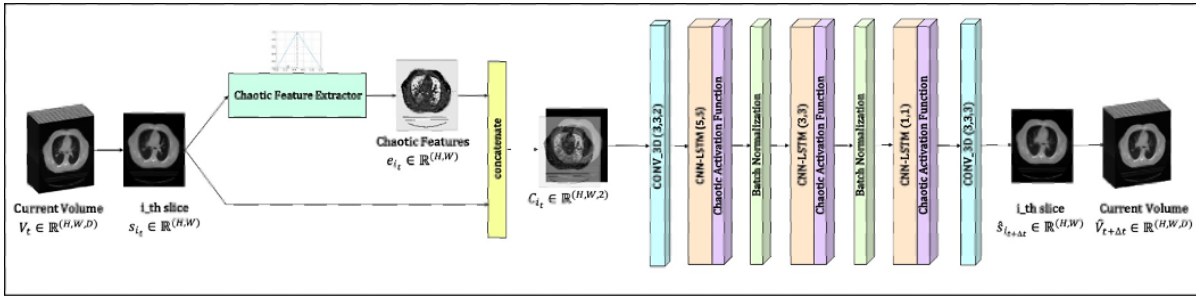


Figure 1: The architecture of the Chaotic Convolutional LSTM Network (CCLSTMNet).

### 3.2.3 Chaotic Activation Function

In recent studies, oscillatory activation functions have shown promise in improving the gradient process and minimizing the network size (Noel et al., 2021). Traditional activation functions such as the sigmoid, rectified linear unit (ReLU), and hyperbolic tangent (Tanh) come with their respective benefits and drawbacks. The vanishing gradient problem is a challenge for sigmoid and Tanh functions, slowing the learning process, whereas ReLU can result in dead neurons when many neurons' activation values are zero.

A chaos-based activation function was proposed to better mirror the neuronal structure of the brain, incorporating the sigmoid function with the logistic map to induce chaos (Reid and Ferens, 2021). The logistic map is utilized for its capacity to create chaotic behavior.

The sigmoid function, bounded between zero and one, ensures the logistic map's input remains within the required range, defined as follows:

$$\text{Sigmoid}(x) = \frac{1}{1 + e^{-x}} \quad (3)$$

Subsequently, the output of the sigmoid function serves as the input to the logistic map:

$$\text{LogisticMap}(x) = r \cdot x \cdot (1 - x) \quad (4)$$

where  $r$  is the excitatory rate of a neuron. This composite function constitutes the chaos-based activation function, instilling a chaotic dynamic in the network's function.

### 3.3 Implementation Details

The code implementation was performed using the Keras library in Python, with the computational environment provided by Google Colaboratory Pro (Colab Pro), a cloud-based Jupyter Notebook service. A batch size of one was utilized. We started with a learning rate of 0.001, implementing a reduction strategy when the loss ceased improving for a duration of five epochs. The neural network was trained using the

Mean Squared Error (MSE) loss function to minimize the difference between the predicted outputs and the ground truth data. The optimization of the network weights was conducted using the Adam optimizer.

Considering computational efficiency, the input images were resized to a resolution of  $160 \times 160$ . The 'leave one patient out' cross-validation method was employed for model evaluation. This involved using data from one patient as the test set and the rest for training, iterating through each patient. The initial neural activity for the GLS neurons was set at 0.7, with the parameter  $b$  in the GLS map from Equation 2 set to 0.467.

## 4 EXPERIMENTAL RESULTS

In this section, we present the experimental setup used to evaluate the respiratory motion prediction framework, with comparisons to state-of-the-art methods. To examine how each component contributes to the framework's overall performance, a set of experiments is presented. We achieve this by conducting an ablation study and experiments focusing on individual components such as chaotic feature extraction and chaotic activation function. Additionally, we compare our method with other approaches that generate images.

### 4.1 Experimental Designs

In our study, we employed the CREATIS dataset, which consists of ten 3D volumes per patient, representing distinct phases of the respiratory cycle for six patients. The imaging was conducted with a 16 Slice Brilliance CT Big Bore Oncology™ configuration from Philips (Vandemeulebroucke et al., 2007). Axially sliced volumes were saved as reference images. The number of images in axial view for each patient is outlined in Table 1. In total, 10090 CT slices were compiled for the six patients. To manage computation costs, these slices were resized to  $160 \times 160$

in the preprocessing phase.

Table 1: Number of slices per volume.

| Patient   | Number of slices per volume |
|-----------|-----------------------------|
| Patient 1 | 141                         |
| Patient 2 | 169                         |
| Patient 3 | 170                         |
| Patient 4 | 187                         |
| Patient 5 | 181                         |
| Patient 6 | 161                         |

The leave-one-patient-out (LOPO) cross-validation method was applied to evaluate the model’s robustness, with a training set composed of the data from five patients and the sixth patient’s data serving as the test set. This procedure was cycled through each patient to complete the validation process.

In this paper, we employ three evaluation metrics to assess the performance of our proposed model: Root Mean Squared Error (RMSE), Structural Similarity Index (SSIM), and Peak Signal-to-Noise Ratio (PSNR).

This metric measures the difference between predicted and actual values. When applied to image processing, it measures how closely a predicted image matches the original image. A lower RMSE indicates less error between the predicted and original images, which means the predicted image is more accurate. RMSE is calculated using Equation 5:

$$\text{RMSE}(x, y) = \sqrt{\frac{\sum_{i=1}^M \sum_{j=1}^N (x(i, j) - y(i, j))^2}{MN}} \quad (5)$$

where  $x$  and  $y$  represent the ground truth and the predicted images, respectively, with  $M$  representing the number of rows and  $N$  representing the number of columns in each image.

SSIM measures the similarity between two images by comparing their structural information, luminance, and contrast. It provides a score ranging from -1 to 1, with a higher score indicating greater similarity between the predicted and original images. SSIM is defined as per Equation 6:

$$\text{SSIM}(x, y) = \frac{(2\mu_x\mu_y + c_1)(2\sigma_{xy} + c_2)}{(\mu_x^2 + \mu_y^2 + c_1)(\sigma_x^2 + \sigma_y^2 + c_2)} \quad (6)$$

where  $\mu_x$  and  $\mu_y$  are the average pixel values of images  $x$  and  $y$ ,  $\sigma_x^2$  and  $\sigma_y^2$  are the variances of  $x$  and  $y$ , and  $\sigma_{xy}$  is the covariance of the images. The constants  $c_1$  and  $c_2$  are small stabilizers to prevent division by zero.

PSNR is another measure of image quality evaluation, which quantifies the quality of a reconstructed image or video by comparing it to the original, undistorted version. A higher PSNR value suggests less

distortion. PSNR is obtained from Equation 7:

$$\text{PSNR}(x, y) = 10 \log_{10} \left( \frac{\text{MAX}_I^2}{\text{MSE}(x, y)} \right) \quad (7)$$

where  $\text{MAX}_I$  is the maximum possible pixel value of the image, and MSE is the mean squared error as calculated in Equation 8.

$$\text{MSE}(x, y) = \frac{1}{MN} \sum_{i=1}^M \sum_{j=1}^N (x(i, j) - y(i, j))^2 \quad (8)$$

## 4.2 Results

In Table 2, we present the quantitative results obtained from the Chaotic ConvLSTM network for each patient in terms of RMSE, SSIM, and PSNR. Also, the weighted average of these results is presented. Figure 2 shows the RMSE and SSIM between ground truth and predicted slices across the different patients. Figure 3 shows some examples of the model output, ground truth, and their difference during the ten phases.

Table 3 shows the comparison results of the respiratory motion prediction algorithms using ConvLSTM and CGAN on the CREATIS dataset. Compared to other algorithms, the proposed strategy accuracy has been improved, and the training time has been reduced.

## 4.3 Ablation Study

In order to better understand the role and contribution of each module in our framework, an ablation study was performed. Different configurations of the proposed model have been deployed. The baseline version of the model includes a sequence of ConvLSTM with a chaotic activation function and a CNN module. This means that the model attempts to learn how to generate volumes directly by generating slices without considering chaotic features. Table 4 shows the results of the ablation study, evaluating each configuration based on the quantitative metrics.

## 5 DISCUSSION

In this paper, we introduced a Chaotic ConvLSTM network designed for predicting 3D CT scan slices from preceding scans. The innovation of this model lies in harnessing chaotic features inherent in respiratory signals, leading to notable enhancements in learning speed and prediction accuracy compared to existing methods. Such improvements underscore the

Table 2: Quantitative metrics result.

| Patient              | RMSE                                    | SSIM              | PSNR            |
|----------------------|---|-------------------|-----------------|
| Patient 1 experiment | $4 \times 10^{-3}$                      | 0.995             | 48.09           |
| Patient 2 experiment | $5 \times 10^{-3}$                      | 0.994             | 44.93           |
| Patient 3 experiment | $8 \times 10^{-3}$                      | 0.988             | 41.49           |
| Patient 4 experiment | $7 \times 10^{-3}$                      | 0.992             | 43.13           |
| Patient 5 experiment | $5 \times 10^{-3}$                      | 0.993             | 45.17           |
| Patient 6 experiment | $5 \times 10^{-3}$                      | 0.993             | 45.53           |
| Weighted average     | $6 \times 10^{-3} \pm 1 \times 10^{-3}$ | $0.993 \pm 0.002$ | $44.60 \pm 1.6$ |

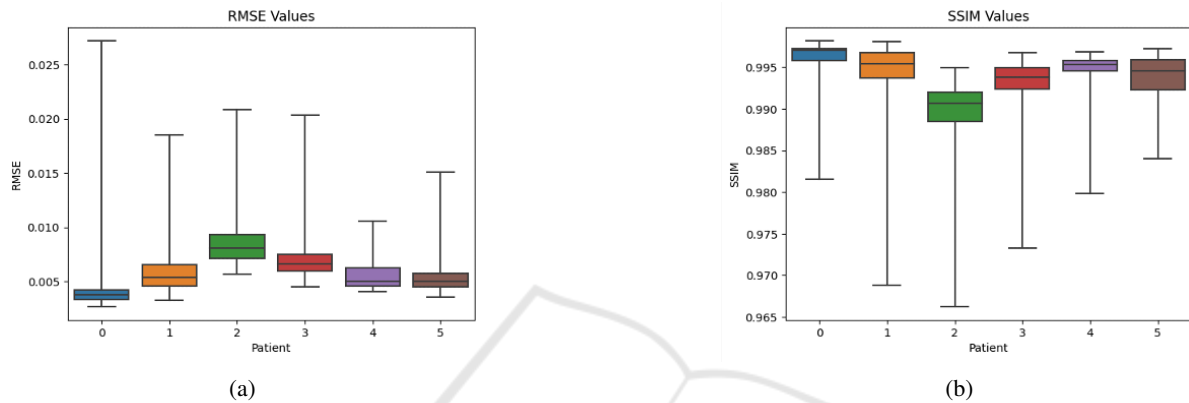
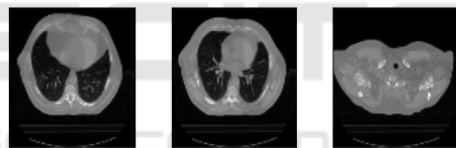
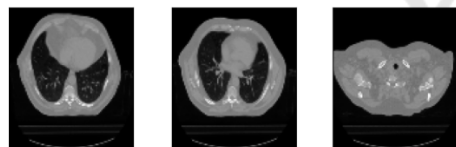


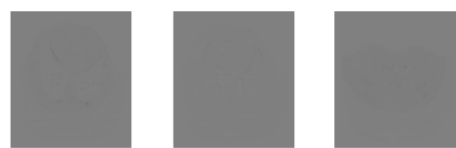
Figure 2: (a) RMSE values obtained for 6 patients. (b) SSIM values obtained for 6 patients.



(a) Reference slices.



(b) Predicted slices.



(c) Difference between reference and predicted slices.

Figure 3: The predicted pulmonary motion. The first row represents the reference slices; the second row represents the predicted slices, and the third row represents the difference between the reference image and the predicted image.

model’s potential for clinical application, particularly in optimizing radiation therapy through respiratory motion prediction.

Given the chaotic nature of respiratory signals, our approach employs chaotic feature extraction, mimicking the complex firing patterns observed in neural structures. This strategy not only refines the prediction process but also contributes to the precision of radiation therapy, potentially increasing its efficacy.

The process of generating images, a core component of our method, is inherently non-invasive. By predicting 4D CT scans within a respiratory cycle, our approach offers detailed insights into organ motion, encompassing anatomical details and tissue characteristics beyond mere motion tracking. This wealth of information holds significant promise for enhancing treatment planning and diagnostic accuracy.

Recent advances in medical imaging technologies have significantly broadened our capabilities in diagnosing and treating complex health conditions. Among these, 4D CT imaging stands out for its comprehensive visualization of organ and tissue dynamics. Nonetheless, the application of 4D CT imaging is not without its drawbacks, notably the high radiation exposure required and the potential for image distortion due to the compilation of multiple CT scans over time.

Our proposed Chaotic ConvLSTM network presents a viable alternative, especially in settings lacking advanced 4D CT imaging capabilities. Its ability to simulate 4D imaging from a single 3D CT scan could substantially reduce radiation expo-

Table 3: Performance comparison of video next frame prediction models on a 4D MRI video.

| Model                                       | RMSE              | SSIM              |
|---|-------------------|-------------------|
| cGAN(Isola et al., 2017)                    | 0.015             | 0.937             |
| ConvLSTM(Nabavi et al., 2020)               | 0.009             | 0.943             |
| ConvLSTM(Ghasemi and Samadi Miandoab, 2022) | 0.012             | 0.988             |
| Proposed Method                             | $0.006 \pm 0.001$ | $0.993 \pm 0.002$ |

Table 4: Quantitative metrics comparison between different configurations.

| Model                           | RMSE ( $\times 10^{-3}$ ) | SSIM              |
|---------------------------------|---------------------------|-------------------|
| ConvLSTM                        | $744 \pm 163$             | 0.959             |
| Baseline (ConvLSTM + CAF)       | $653 \pm 152$             | $0.992 \pm 0.002$ |
| Proposed (ConvLSTM + CAF + CFE) | $626 \pm 141$             | $0.993 \pm 0.002$ |

sure and eliminate the distortions and artifacts typical of traditional 4D CT reconstructions. These advantages are particularly appealing for radiotherapy centers with limited access to cutting-edge imaging technology, offering a cost-effective yet efficient solution.

Furthermore, the comparative analysis of error rates and the fidelity of generated images to their ground truth counterparts confirm the superiority of our model over traditional ConvLSTM-based approaches. This efficacy stems from our model’s unique integration of chaotic dynamics, enhancing its ability to predict pulmonary motion with remarkable accuracy.

In light of these findings, our work contributes to the ongoing evolution of medical imaging and predictive modeling. By leveraging the chaotic patterns inherent in biological systems, we offer a novel perspective on motion prediction that could significantly impact the field of radiation therapy and beyond. Future work will aim to expand the application of chaotic feature extraction and explore its potential in other areas of medical imaging and treatment planning, paving the way for broader clinical adoption.

## 6 CONCLUSIONS

In this study, we developed and presented a novel Chaotic Convolutional LSTM Network aimed at enhancing the accuracy of respiratory motion prediction for radiation therapy planning. This method predicts each subsequent CT slice based on the preceding one. This approach, tested on the CREATIS dataset, underscores the method’s superiority over traditional 4D CT-generating techniques by offering significant improvements in prediction accuracy.

The promising outcomes of this research highlight not just the methodological advancements but also the potential for substantial clinical impact, particularly in the field of radiation therapy where precise

tumor targeting is critical. The reduced error rates and the method’s non-invasive nature represent significant steps forward in the pursuit of safer, more effective treatment strategies.

Looking ahead, our research opens several avenues for further investigation and application. A key direction for future work involves validating the proposed Chaotic ConvLSTM network against dynamic breathing lung phantoms, a crucial step towards confirming its applicability and effectiveness in real-world clinical settings. Additionally, exploring the integration of this network into existing radiation therapy planning systems could provide actionable insights into its operational benefits and challenges.

The successful application of chaotic characteristics in respiratory motion prediction underscores a promising path for future investigations. We plan to explore the potential of the Chaotic ConvLSTM network in modeling physiological processes with similar chaotic dynamics. This exploration aims to broaden the utility of our approach, offering a comprehensive tool for analyzing and predicting complex physiological behaviors that exhibit chaotic properties. By focusing on these areas, we intend to deepen our understanding of chaotic phenomena in biology and their implications for medical imaging and diagnostics.

In conclusion, the Chaotic ConvLSTM network represents an advancement in the predictive modeling of respiratory motion. Its development not only contributes to the body of knowledge in medical imaging and computational biology but also sets the stage for groundbreaking applications in personalized medicine and advanced healthcare delivery.

## ACKNOWLEDGEMENTS

The authors are grateful to Léon Bérard Cancer Center and CREATIS Laboratory, Lyon, for sharing their

imaging data.

## REFERENCES

- Balakrishnan, H. N., Kathpalia, A., Saha, S., and Nagaraj, N. (2019). Chaosnet: A chaos based artificial neural network architecture for classification. *Chaos: An Interdisciplinary Journal of Nonlinear Science*, 29(11).
- Bukhari, W. and Hong, S. (2014). Real-time prediction and gating of respiratory motion using an extended kalman filter and gaussian process regression. *Physics in Medicine & Biology*, 60(1):233.
- Ghasemi, Z. and Samadi Miandoab, P. (2022). Feasibility study of convolutional long short-term memory network for pulmonary movement prediction in ct images. *Journal of Biomedical Physics and Engineering*.
- Gottwald, G. A. and Melbourne, I. (2004). A new test for chaos in deterministic systems. *Proceedings of the Royal Society of London. Series A: Mathematical, Physical and Engineering Sciences*, 460(2042):603–611.
- Harikrishnan, N. B. and Nagaraj, N. (2019). A novel chaos theory inspired neuronal architecture. In *2019 Global Conference for Advancement in Technology (GCAT)*, pages 1–6. IEEE.
- Isola, P., Zhu, J.-Y., Zhou, T., and Efros, A. A. (2017). Image-to-image translation with conditional adversarial networks. In *Proceedings of the IEEE conference on computer vision and pattern recognition*, pages 1125–1134.
- Kai, J., Fujii, F., and Shiinoki, T. (2018). Prediction of lung tumor motion based on recurrent neural network. In *2018 IEEE International Conference on Mechatronics and Automation (ICMA)*, pages 1093–1099. IEEE.
- Lee, S. J., Motai, Y., and Murphy, M. (2011). Respiratory motion estimation with hybrid implementation of extended kalman filter. *IEEE Transactions on Industrial Electronics*, 59(11):4421–4432.
- Lin, H., Shi, C., Wang, B., Chan, M. F., Tang, X., and Ji, W. (2019). Towards real-time respiratory motion prediction based on long short-term memory neural networks. *Physics in Medicine & Biology*, 64(8):085010.
- Lotter, W., Kreiman, G., and Cox, D. (2016). Deep predictive coding networks for video prediction and unsupervised learning. *arXiv preprint arXiv:1605.08104*.
- McCall, K. and Jeraj, R. (2007). Dual-component model of respiratory motion based on the periodic autoregressive moving average (periodic arma) method. *Physics in Medicine & Biology*, 52(12):3455.
- Michalski, D., Huq, M., Bednarz, G., Lalonde, R., Yang, Y., and Heron, D. (2014). Su-e-j-261: Statistical analysis and chaotic dynamics of respiratory signal of patients in bodyfix. *Medical Physics*, 41(6Part10):218–218.
- Nabavi, S., Abdoos, M., Moghaddam, M. E., and Mohammadi, M. (2020). Respiratory motion prediction using deep convolutional long short-term memory network. *Journal of Medical Signals & Sensors*, 10(2):69–75.
- Noel, M. M., Trivedi, A., Dutta, P., et al. (2021). Growing cosine unit: A novel oscillatory activation function that can speedup training and reduce parameters in convolutional neural networks. *arXiv preprint arXiv:2108.12943*.
- Rehailia-Blanchard, A., De Oliveira Duarte, S., Bauray, M., Auberdiaac, P., Diard, A., Brun, C., Talabard, J., Rancoule, C., Magné, N., et al. (2019). Use of 4d-ct: Main technical aspects and clinical benefits. *Cancer Radiotherapie: Journal de la Societe Francaise de Radiotherapie Oncologique*, 23(4):334–341.
- Reid, S. and Ferens, K. (2021). A hybrid chaotic activation function for artificial neural networks. In *Advances in Artificial Intelligence and Applied Cognitive Computing: Proceedings from ICAI'20 and ACC'20*, pages 1097–1105. Springer.
- Rostampour, N., Jabbari, K., Esmaceli, M., Mohammadi, M., and Nabavi, S. (2018). Markerless respiratory tumor motion prediction using an adaptive neuro-fuzzy approach. *Journal of medical signals and sensors*, 8(1):25.
- Ruan, D. (2010). Kernel density estimation-based real-time prediction for respiratory motion. *Physics in Medicine & Biology*, 55(5):1311.
- Shi, X., Chen, Z., Wang, H., Yeung, D.-Y., Wong, W.-K., and Woo, W.-c. (2015). Convolutional lstm network: A machine learning approach for precipitation nowcasting. *Advances in neural information processing systems*, 28.
- Siegel, R. L., Miller, K. D., Fuchs, H. E., and Jemal, A. (2022). Cancer statistics, 2022. *CA: a cancer journal for clinicians*, 72(1):7–33.
- Sun, W., Jiang, M., Ren, L., Dang, J., You, T., and Yin, F. (2017). Respiratory signal prediction based on adaptive boosting and multi-layer perceptron neural network. *Physics in Medicine & Biology*, 62(17):6822.
- Vandemeulebroucke, J., Sarrut, D., Clarysse, P., et al. (2007). The popi-model, a point-validated pixel-based breathing thorax model. In *XVth international conference on the use of computers in radiation therapy (ICCR)*, volume 2, pages 195–199.